T. J. Jackson, C. E. Gough, *Nature* **340**, 210 (1989).
52. R. F. Kiefl *et al.*, *Phys. Rev. Lett.* **64**, 2082 (1990).
53. W. E. Pickett, H. Krakauer, R. E. Cohen, *Physica B* **165 & 166**, 1055 (1990).
54. This paper is dedicated to the memory of Stephan Berko, a good friend and a pioneer in the positron spectroscopy of Fermi surfaces. W.E.P. acknowledges the hospitality of the Cavendish Laboratory, Cambridge, England, where much of this paper was written. We thank J. W. Serene for thoughtful comments on the manuscript. We acknowledge the support of two national supercomputer centers where most of our calculations have been carried out: the Cornell National Supercomputing Facility (IBM 3090 computer grants to W.E.P., H.K., D.J.S.) and the National Center for Supercomputing Applications (Cray 2 grant to R.E.C.). H.K. was supported by NSF grant no. DMR-90-22588, W.E.P. and D.S. were supported by the Office of Naval Research, and R.E.C. acknowledges support from the Carnegie Institution of Washington.

Molecular Code for Cooperativity in Hemoglobin

GARY K. ACKERS,* MICHAEL L. DOYLE, DAVID MYERS, MARGARET A. DAUGHERTY

Although tetrameric hemoglobin has been studied extensively as a prototype for understanding mechanisms of allosteric regulation, the functional and structural properties of its eight intermediate ligation forms have remained elusive. Recent experiments on the energetics of cooperativity of these intermediates, along with assignments of their quaternary structures, have revealed that the allosteric mechanism is controlled by a previously unrecognized symmetry feature: quaternary switching from form T to form R occurs whenever heme-site binding creates a tetramer with at least one ligated subunit on each dimeric half-molecule. This "symmetry rule" translates the configurational isomers of heme-site ligation into six observed switchpoints of quaternary transition. Cooperativity arises from both "concerted" quaternary switching and "sequential" modulation of binding within each quaternary form, T and R. Binding affinity is regulated through a hierarchical code of tertiary-quaternary coupling that includes the classical allosteric models as limiting cases.

A MAJOR DISCOVERY OF MODERN BIOCHEMISTRY WAS THAT proteins act as molecular switches to regulate metabolic reactions (*1, 2*). Intracellular control of enzymic activity is often brought about by multimeric assemblies of enzyme subunits that undergo changes in the conformation (tertiary structure) and the arrangement of intersubunit contacts (quaternary structure) in response to the binding of substrates and other "regulatory" molecules. These alterations in protein structure either enhance or diminish binding affinities and thus regulate the concentrations of product. Cooperativity, or "self-regulation," is manifested when the binding of a ligand species alters the affinity for subsequent binding of the same ligand. The protein brings this about by acting as a transducer of free energy: favorable increases in binding energy are "paid for" by (unfavorable) decreases in the free energies of subunit interaction and conformational rearrangement within the protein itself. This transduction of free energy between binding sites and conformational states is reciprocal; after ligand dissociation the original protein structure is restored.

Studies on the structural and functional properties of tetrameric hemoglobin have had a pivotal role in the development of concepts to explain cooperativity and regulation by allosteric enzymes and other multisubunit proteins. The hemoglobin molecule was awarded the rank of "honorary enzyme" by Monod, in recognition that it displays the essential features of allosteric regulation yet maintains the comparative simplicity desired in a model system. Hemoglobin thus had a significant role in the development of the classical theories for allosteric regulation during the 1960s by Monod *et al.* (MWC) (*3*) and by Koshland *et al.* (KNF) (*4*). These models were based on concepts of "concerted" (all or none) versus "sequential" (ligand-induced) processes, respectively. They have provided sharply contrasting frameworks for understanding how regulatory behavior can arise from protein conformational changes coupled to subunit interactions and ligand binding (Fig. 1).

Hemoglobin has also played a major role in the progress toward understanding the detailed structural basis of allosteric regulation, beginning with the pioneering work of Perutz on crystallographic structures of unligated and fully ligated tetramers [see (*5*) for an extensive review of allosteric structures]. The hemoglobin molecule continues to be the object of an immense range of studies on the structural, dynamic, spectroscopic, energetic, clinical, and engineering issues of protein structure and function, for which no attempt at review will be made here. In this article we describe recent findings on properties of the intermediate-state species (partially ligated tetramers) that shed new light on the origins of hemoglobin cooperativity (*6–12*) and the rules whereby heme-site ligation generates cooperativity through tertiary and quaternary switches.

How can it be that the allosteric mechanism of hemoglobin is not completely understood, given the vast amount of effort that has gone into the problem over a number of years? Highly cooperative systems greatly suppress the populations of molecular forms that lie on the pathway between the initial and final states, which makes it extremely difficult to study the properties that may reveal features critical to an understanding of the overall mechanism. The same "conspiracy" is encountered in attempts to understand the mechanisms of protein folding and of nucleated polymerization by filamentous protein assemblies. The recent discovery that hemoglobin quaternary structure is controlled by the specific configuration of ligated subunits within the tetrameric molecule (7) could only arise from studies on the different intermediate species at each degree of ligation.

The authors are in the Department of Biochemistry and Molecular Biophysics, Washington University School of Medicine, St. Louis, MO 63110.

*To whom correspondence should be addressed.

Hemoglobin Structure and Motion

Tetrameric hemoglobin ($\alpha_2\beta_2$) is an assembly of two asymmetric dimers ($\alpha\beta$) (Fig. 2) (*5, 13–16*). The dimers assemble in either of two ways to form quaternary structure T (tense, also called "deoxy") or quaternary structure R (relaxed, also called "oxy"). After the binding of a heme-site ligand, each α or β subunit undergoes a change in tertiary structure (from t to r). These tertiary transitions of the individual subunits promote the quaternary T→R transition, leading to the altered arrangement between the dimeric halves of the molecule. This arrangement requires a global shift of the dimer interfaces (*14*), not just an alteration of subunit shape and of intersubunit bonds (*17*). The interface within each dimer ($\alpha^1\beta^1$ and $\alpha^2\beta^2$) undergoes motion on a smaller scale and is, by convention, considered "tertiary" rather than "quaternary." Through a combination of tertiary and quaternary motions that accompany ligand binding, a tetramer originally in unligated T becomes energetically more stable in quaternary R when all four subunits contain ligated hemes. Thus, some of the local heme-site binding energy has been used to pay for the structural rearrangement that forms quaternary R.

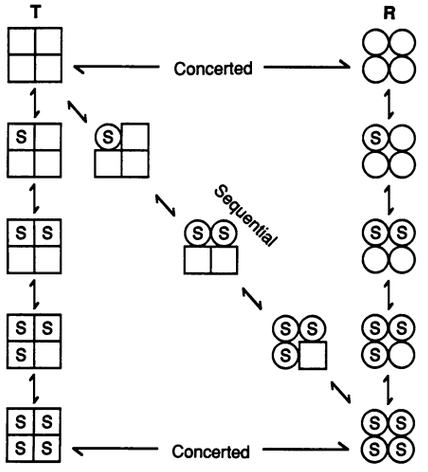

Fig. 1. Contrasting ways of generating cooperativity according to the "concerted" MWC (*1*) and "sequential" KNF (*2*) models. Each subunit has two distinct tertiary conformations, one with higher ligand affinity for ligand S than the other. In the "concerted" model, the oligomeric molecule is postulated to exist in only two global conformations, T and R. In quaternary T, all subunits have the low-affinity tertiary conformation t (squares); in quaternary R, they all have the high-affinity conformation r (circles). The fully unligated oligomer favors T, whereas the R form predominates in fully ligated molecules. Changes in conformation of individual subunits occur in a "concerted" or "all or none" fashion so that the oligomer is always symmetrical. The "sequential" or "ligand-induced" (KNF) model (*2*) is indicated by the diagonal, where species proceed through a sequence of intermediate conformations. Ligand binding induces a change to the high-affinity conformation (r) in each ligated subunit, whereas the unligated subunits retain their low-affinity conformations (t). Altered pairwise contacts of each ligated subunit with its neighbors influence the neighboring subunit's tendency to bind the next ligand and to switch to the high-affinity form. The sequential model can account for both positive or negative cooperativity (that is, binding a ligand diminishes the affinity for subsequent binding), whereas the concerted model can only accommodate positive cooperativity. [Adapted from (*4*)]

The exact nature of the structural rearrangements being "paid for" has been a subject of much research and contrasting views. The KNF and MWC approaches both emphasize the role of subunit-subunit interactions but use radically different rules (Fig. 1). In the MWC model a set of favorable intersubunit bonds are held responsible for constraining the unligated tetramer into its low-affinity T structure (an effect termed "quaternary constraint"). A ligated subunit within T is forced to remain in its "unligated" tertiary t conformation ("conservation of symmetry"), giving it a reduced binding energy compared to the same subunit in quaternary R (*18*). After several ligands are bound, the cumulative unfavorable free energy is sufficiently high that the tetramer becomes energetically more favorable to the R structure. An "all or none" transition from T to R breaks the (noncovalent) bonds of "quaternary constraint," leading to the "relaxed" high-affinity R structure, with all subunits in their tertiary r forms. In contrast, the sequential KNF model requires mixed conformational states and thus by necessity violates the MWC symmetry constraint.

Crystallographic and spectroscopic studies of doubly ligated hemoglobins in quaternary T (*19–23*) have shown that the ligated subunits do, in fact, assume tertiary r structures in violation of the MWC symmetry rule. The subunits adopt structures t or r, depending primarily on the distance from the heme plane of the proximal histidine, which is normally coordinated to the heme [Fe(II)] atom. After binding a ligand, the metal ion moves into the plane of the heme as a "trigger" for the allosteric transitions. It carries residues of

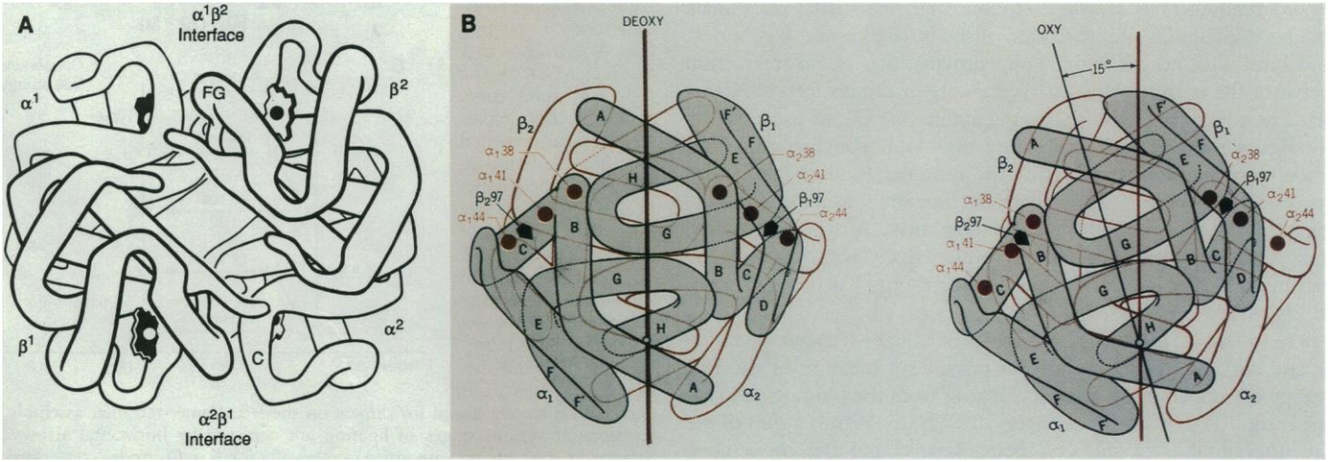

Fig. 2. Subunit structure and motion of tetrameric hemoglobin. (**A**) Quaternary assembly of the two dimeric halves $\alpha^1\beta^1$ (left) and $\alpha^2\beta^2$ (right) to form the $\alpha^1\beta^2$ interface. The $\alpha^1\beta^1$ dimer is in the deoxy conformation, whereas the $\alpha^2\beta^2$ dimer is in the oxy conformation. The interfaces $\alpha^1\beta^2$ and $\alpha^2\beta^1$ are labeled where sliding contacts between FG corners and C helices shift in the quaternary transition. (**B**) Quaternary structure change of the tetramer from deoxy T (left) to oxy R (right). A 15° rotation of the $\alpha^1\beta^1$ dimer (front, shaded) occurs relative to the identical fixed $\alpha^2\beta^2$ dimer (back) at the hinge point, producing contact dislocation of 7 Å at the maximum (top). The β97 histidine side-chain (black arrow) occupies alternative positions in the two quaternary structures, interlocking between residues α41 and α44 (deoxy) or between α38 and α41 (oxy) (reddish-brown circles). Tight contacts in the $\alpha^1\beta^1$ and $\alpha^2\beta^2$ dimers are principally between G helices. [Figures © Irving Geis]

the F helix, leading to cramped FG corners that impact on the neighboring subunits. The role of this active structure within each subunit (designated the "allosteric core") has been analyzed in detail by Karplus and co-workers (*24*).

A stereochemical model, developed by Perutz (*25*) to explain the hemoglobin mechanism, identified the two end-state crystallographic structures with the T and R concepts of MWC but also incorporated the ligand-induced alteration of intersubunit bonds, which plays a key role in the KNF approach. A number of other models have been proposed that in various ways also hybridize the basic KNF and MWC concepts (*26–30*). They represent a diverse range of rules and levels of structural detail.

Important insights into the structural nature of heme-site cooperativity have come from the nuclear magnetic resonance (NMR) studies of Ho and co-workers (*31–35*). They found that tertiary and quaternary changes during the course of oxygenation were inconsistent with a strictly two-state mechanism. New understanding of the nature and localization of "allosteric energy" has come from elegant hydrogen-exchange techniques developed by Englander and co-workers (*36*).

Energetics of Cooperativity and Subunit Interaction

The concept of cooperativity arising from the ligand-driven modulation of intersubunit interactions virtually demands that these processes should be "dissected" by experimental determination of the energetics of subunit interactions at the different stages of heme-site binding [see Noble (*37*) and Weber (*38*)]. A program of research aimed toward this goal has been carried out by our laboratory since 1974 (*39–43*). Because cooperativity is mediated through interactions at the intersubunit contacts within the tetrameric molecule, subunit dissociation has proven to be a powerful quantitative tool for probing the energetic components of cooperativity. The strategy uses a combination of techniques that simultaneously analyze the linked reactions of binding and assembly. Oxygen-binding techniques developed by Imai (*44*) and Gill and co-workers (*45*) have been especially valuable to these studies, as have kinetic methods pioneered by Gibson (*46*).

The major manifestations of cooperativity found in heme-site ligand binding (Fig. 3) are as follows: (i) dissociated αβ dimers exhibit high affinity, equal to that of the isolated α and β subunits, and bind with no detectable cooperativity (that is, no interaction between the α and β sites); (ii) assembly of dimers into tetramers leads to a large reduction in overall affinity for O_2, as indicated by the rightward shift with increasing hemoglobin concentration (and fraction of tetramers); and (iii) the tetramer binds ligands with successively increasing affinity over the four steps, as reflected in the sigmoid shape of the rightmost binding curve. A diagram of these linked reactions and a "thermodynamic ledger" showing how the various processes are reflected in the free-energy balance are shown in Fig. 3B.

The difference between free energies of a dimer-tetramer assembly at any two stages of oxygenation provides a measure of the free energy of cooperative interaction arising from the binding of O_2 at the hemes. The binding free energy at each step is thus a sum of the intrinsic affinities of the sites being ligated and the cooperative free-energy term for that step (the "energy cost" of protein structural rearrangement). The free-energy terms on the right-hand side of Fig. 3B pertain to the same experimental conditions as the binding curves in Fig. 3A. The bottom line shows that the free-energy increments spent by the protein over all four stages of ligation to pay for the deviations from intrinsic subunit affinity sum to 6.3 kcal (the "total cooperative free energy" $^{41}\Delta G_c$). It should be noted that $^{41}\Delta G_c$ is the underlying energy source for modulation of binding affinities; it is not the same as the variations in the tetrameric constants, which are a more common measure of cooperativity (*47*).

Dissection of cooperative interactions by this approach has been carried out with normal hemoglobin over a wide range of conditions and with mutant and chemically modified molecules (*39–43, 48*). Results of these and other studies on hemoglobin oxygenation (*44, 49*) have defined the energetics of cooperativity at different stages (that is, with zero to four oxygens bound) and have delineated the linkages to other physiological regulators of the hemoglobin system, including protons, Cl^- ions, 2,3-diphosphoglycerate, and CO_2. However, in spite of these advances, direct oxygen-binding studies alone are incapable of resolving properties of the configurational isomers at each stage of binding (for example, the first binding constant does not distinguish between α or β). Resolution of the energetics of cooperativity for the ten microstates of ligation has required the development of an approach discussed below.

The Intermediate Ligation Species

During the course of ligand binding, the tetramer can form ten different molecular species that constitute the particular structural combinations of ligated and unligated subunits (Fig. 4). Each species reflects in principle a different combination of structurally altered intersubunit contacts within each quaternary structure T and R. Direct analysis of the properties of the eight partially oxygenated

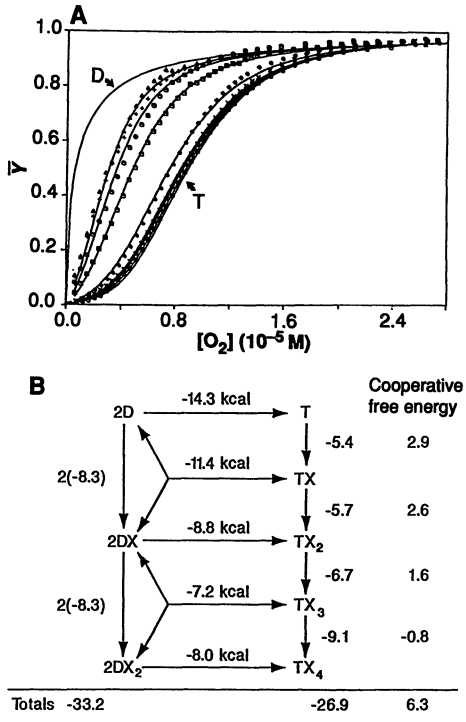

Fig. 3. Cooperativity in hemoglobin O_2-binding. (**A**) Binding isotherms at decreasing hemoglobin concentrations (right to left). The rightmost curve pertains to tetramers (T) (n = 3.3), and the leftmost solid curve is for dissociated $\alpha^1\beta^1$ dimers (D) (n = 1.0). Intermediate curves are at hemoglobin concentrations ranging from 4×10^{-8} M to 1×10^{-4} M (*40*). The rightmost solid curve simultaneously represents the experimental tetramer binding-constants and the prediction according to the microstate values of Table 1 (see Fig. 7). (**B**) Linkage diagram showing free-energy components of the cooperative mechanism. Binding of ligand species X to tetramers is depicted on the right and for dimers on the left. Dimer-tetramer assembly reactions at various stages of ligation are depicted by horizontal arrows. Standard Gibbs energies are given numerically for X = O_2 under conditions of data in (A). Reactions are taken left to right and top to bottom. Cooperative free energies (right) are the net energetic cost for binding to the assembled tetramers and reflect protein structural alterations that accompany the bindings. Quaternary assembly results in decreased affinity for the first binding step, which is "paid for" by 2.9 kcal/mol of "free energy of protein structural rearrangement." [(A) reprinted from (*40*) with permission, © 1976 American Chemical Society]

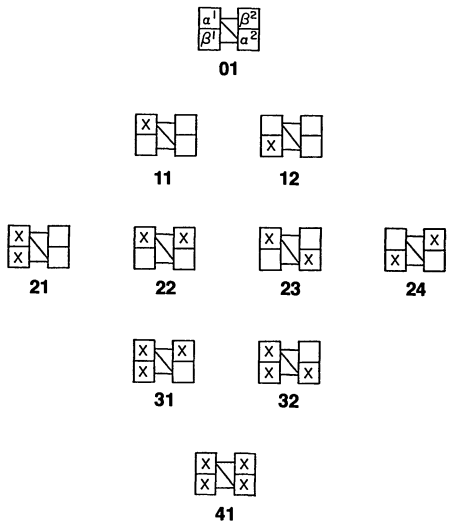

Fig. 4. Topographic representation of the ten ligation species of tetrameric hemoglobin. The index **ij** denotes the particular species **j** among those with **i** ligands bound (**i** = **0** to **4**; **j** = **1** to **4**). Ordering of species with respect to **j** is arbitrary. Subunit arrangement is assigned in species **01**.

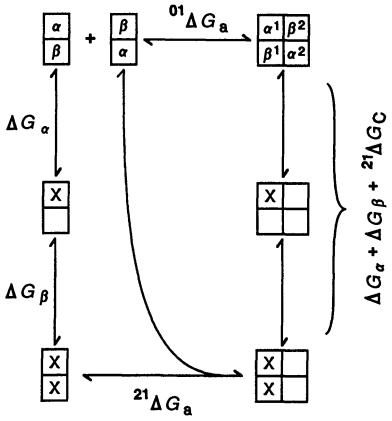

Fig. 5. Thermodynamic linkage between subunit assembly (left to right) and ligand binding (top to bottom). The quantity $^{ij}\Delta G_c$ is the deviation in tetramer-binding free energy from that for ligation of the same sites with their intrinsic free energies: $^{ij}\Delta G_c = {}^{ij}\Delta G_b - p\Delta G_\alpha - q\Delta G_\beta$, where $^{ij}\Delta G_b$ is the free energy for binding **i** moles of ligand to a tetramer to form configuration **ij**. The last two terms are the intrinsic free energies per site for the same reaction in the absence of cooperativity (p and q are the numbers of ligands bound to each type of subunit, and ΔG_α and ΔG_β are the corresponding intrinsic free energies). A finding that $^{21}\Delta G_c = 3$ kcal/mol for species **21** means that when 1 mol of species **01** is reacted with 2 mol of ligand to form species **21**, the standard Gibbs free energy changes by ($\Delta G_\alpha + \Delta G_\beta + 3$) kcal/mol; in the absence of interactions the free-energy change per mole of tetramer would be just $\Delta G_\alpha + \Delta G_\beta$. Because the free energy is a state function, the values around any appropriate cycle must sum to zero. Thus, for doubly ligated species **21**, $^{21}\Delta G_a - {}^{01}\Delta G_a = (\Delta G_\alpha + \Delta G_\beta + {}^{21}\Delta G_c) - (\Delta G_\alpha + \Delta G_\beta)$, where terms in parentheses are ligation free energies of the tetramers and (noncooperative) dimers. This equation reduces to $^{21}\Delta G_c = {}^{21}\Delta G_a - {}^{01}\Delta G_a$. Therefore, an experimental determination of the two assembly free energies provides an evaluation of the cooperative free energy $^{21}\Delta G_c$ without actual measurement of the ligand-binding equilibria.

intermediates has been precluded by the inability either to isolate any of them in pure form or to resolve their individual properties in a mixture (*50*). The difficulties stem from (i) extreme lability and rapid exchange of site-bound O_2 molecules and (ii) dissociation of the tetramers into dimers and reassociation to form tetramers with different arrangements of ligated sites. Efforts to circumvent these problems include (i) the use of tightly bound ligands or metal-substituted hemes that mimic the oxygenated and unligated species (*51–56*), (ii) the use of cryogenic methods to quench and separate these intermediates (*57–60*), (iii) kinetic studies on mixtures of the intermediates (*6, 60*), and (iv) chemical cross-linking of the dimers to prevent dissociation (*33–35, 61*).

Early insights into the global nature of the hemoglobin mechanism came from NMR work on intermediate species **23** and **24** (Fig. 4), in which two identical heme-sites (both α or both β) carry a tightly bound ligand (such as cyanide) or in which the heme iron has been replaced by other metals (such as Co and Mn) so that the "ligation state" of the heme can be stably controlled (*22, 23*). These molecules, which assume the quaternary R form under low-salt conditions, can be shifted to T in high-salt conditions or with organic phosphates, demonstrating that affinity and cooperativity can be controlled by global quaternary structure. These and other properties of species **23** and **24** have frequently been taken as representative of all eight intermediates. In contrast, the new results on these and the other species have revealed surprising additional properties (discussed below).

Resolution of cooperative free-energy distributions. In 1985 Smith and Ackers (*6*) developed a strategy for determining the free energies of subunit assembly (dimers to tetramers) and the cooperativity for each of the ten tetrameric species [see also (*7–11*)]. The problem of ligand lability was circumvented by the use of tightly bound ligands (such as CO or cyanomet) in combination with well-characterized metal-substituted hemes (Mn and Co) that mimic the ligated and unligated structures. To determine cooperativity of ligation processes when the "ligands" are too tight for direct affinity measurement, Smith and Ackers devised an approach that takes advantage of the thermodynamic coupling between the linked reactions of ligation and subunit assembly: cooperativity is measured by the difference in free energies of the assembly reactions for each of the nine ligation species relative to the unligated species **01** (Fig. 5). For six of the eight intermediate species the assembly free energies must be determined in hybrid mixtures (Fig. 6). Techniques adapted for resolving assembly energetics from simultaneous mixtures of hybridized tetramers include kinetic methods (*6, 11*), analytical gel chro-

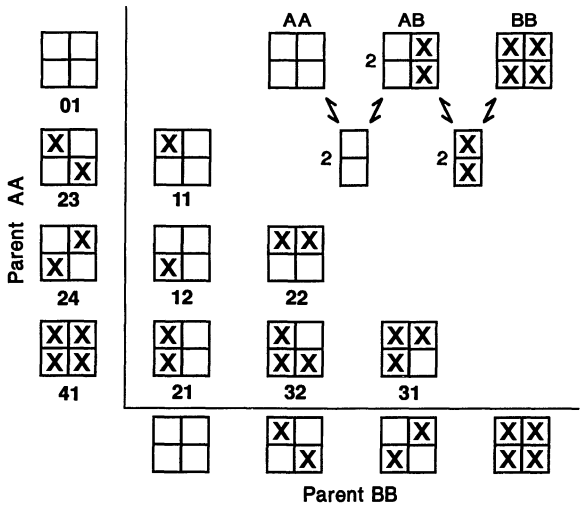

Fig. 6. Hybridization scheme for construction of the six asymmetric species of tetramer by a combination of dimers from the two parent molecules AA or BB. Hybridization occurs through dissociation and reassociation of dimers (upper right). The free energy of assembly for hybrid tetramer AB must be studied in the presence of the parent species AA and BB and of the dissociated dimers. Hybrid-parent mixtures were studied either by the haptoglobin kinetics method (*6*), analytical gel chromatography (*11, 62*), or quantitative cryoisoelectric focusing (*10, 57*). In the latter technique, two parent hemoglobins are mixed in a known ratio and incubated at desired reaction conditions under anaerobic environment. Once equilibrium is attained, the reaction is quenched into a (50:50) solution mixture of ethylene glycol and standard buffer at −25°C, which halts rearrangement of the three tetrameric species. The sample is loaded onto polyacrylamide isoelectric-focusing gels (pH range 6 to 8). Electrophoresis at −25°C separates the three tetrameric species according to their isoelectric point (pI) values. The tubes are scanned at 540 and 420 nm. Fractional areas of the three tetrameric peaks yield the deviation free energy δ, calculated by $\delta = -RT\ln[f_{AB}/2(f_{AA}f_{BB})^{1/2}]$, where f_{AA}, f_{BB}, and f_{AB} are fractional populations of tetramers AA, BB, and AB at equilibrium. Assembly free energy of the hybrid AB is calculated from independently determined values of the parent species: $\delta = \Delta G_{AB} - 1/2(\Delta G_{AA} + \Delta G_{BB})$.

matography (*62, 11*), and low-temperature electrophoresis techniques developed by Perrella, Rossi-Bernardi, and co-workers (*57–60*) and others (*10, 11*).

The initial study on cyanomet hemoglobin (*6*) yielded the surprising result that three discrete free energies of dimer-tetramer assembly exist among the ten ligation species (Table 1). Most remarkable, however, was the finding that doubly ligated molecules exhibit a combinatorial feature: the free energy of the dimer-tetramer assembly depends not only on the number of ligands bound but also on the specific configuration of ligated sites. Subsequent studies provided more accurate assignments of these effects and confirmed the combinatorial nature of the distribution (*58, 7*). Values are given in Table 1 for the cyanomet system Fe(II)/Fe(III)-CN at two pH conditions. Each observed distribution of assembly free energies can be transformed into the corresponding distribution of cooperative free energies and binding free energies (Fig. 5). The data at pH 8.8 show a combinatorial distribution similar to that of the more extensive pH 7.4 set, but with greatly altered spacing of free-energy levels. Extensions of this work (*7, 63*) indicate considerable plasticity of these spacings in response to conditions.

To determine whether a similar combinatorial pattern is also manifested by other heme-site ligands, we determined assembly free energies for all ten species in two other systems (Table 1): (i) Fe(II)/Mn(III), in which the "ligated" subunits contained Mn(III) substituted for Fe in the heme and the unligated subunits contained natural Fe(II) hemes (*8, 52, 54*) and (ii) Co(II)/Fe(II)-CO, in which the unligated subunits contained hemes with Co(II) substituted for Fe and the ligated subunits consisted of normal hemes reacted with CO (*11, 12, 53, 55*). Values were also determined (*8*) for five species in a fourth system, in which Mn(II) served in the unligated hemes [mimicking Fe(II)] and the ligated subunits contained Fe(II)-CO. These diverse ligation systems all exhibit a combinatorial switching pattern similar to that found with cyanomet hemoglobin (including nonidentical cooperative free energies for the doubly ligated species), but with variations in the spacings of energy levels.

Subsequent work has indicated that the cyanomet system behaves as a simplified version of the slightly more general distribution exhibited by Co-substituted hemoglobin (*11, 12*) (Table 1). This work includes the observations that (i) the ten ligation species distribute into five discrete assembly free-energy levels (for example, species **01, 11, 21, 23,** and **41**); (ii) species **11** and **21** occupy separate levels; and (iii) four species of the Co(II)/Fe(II)-CO system exhibit quaternary enhancement; that is, the partially ligated species are more weakly assembled than fully ligated molecules. Quaternary enhancement (Fig. 3) was found in oxygen binding of normal hemoglobin over a wide range of conditions (*42, 49*).

The various ligation systems of Table 1 thus show a common pattern of qualitative relations between the configurations of ligated sites and the ordered distribution of cooperative free energies. It is remarkable that the same characteristic pattern is found even when the magnitudes of energetic spacings differ quantitatively from one ligation system to another. Furthermore, this pattern persists when the energetic spacings are shifted by changing conditions (compare pH 7.4 to pH 8.8, Table 1). These striking common features in the free-energy distribution patterns indicate that site configuration is a controlling factor in determining cooperative free energies.

Comparison with oxygen. To compare cooperativity properties arising from the CO-bound sites of the Co(II)/Fe(II)-CO system with the corresponding effects arising from oxygenation of these sites, the energetics of dimer-tetramer assembly and oxygenation were determined for pure cobaltous hemoglobin Co(II)/Co(II)-O_2 (*12*). These molecules showed free-energy distributions similar to

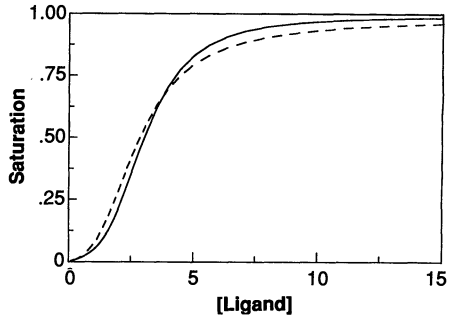

Fig. 7. Correspondence between O_2 and cyanomet ligation. Solid curve is for O_2 binding at pH 8.9 (concentration in micromoles per liter) (*42*). Dashed curve is for cyanomet pH 8.8 data, calculated from values in Table 1 as follows (*9*). The binding isotherm is given by Eq. 1 (below), where [X] is ligand concentration and K_{4i} is the standard Adair constant for binding i ligands. Each of these is a composite: $K_{4i} = K_x^i \Sigma_i g_{ij} \exp[-({}^{ij}\Delta G_c)/RT]$, where K_x is the intrinsic binding constant for the subunits (identical for α and β in this case), g_{ij} is the statistical degeneracy for each microstate, and ${}^{ij}\Delta G_c$ is its cooperative free energy, equal to $({}^{ij}\Delta G_2 - {}^{01}\Delta G_2)$ as described in Fig. 5. The solid curve for O_2 simultaneously represents the experimentally resolved isotherm and that predicted from the assembly free energies of Table 1 plus the intrinsic subunit binding energies of −8.3 kcal. Because these values are not known for the cyanomet system, the predicted binding curve (dashed line) is positioned to have the same median as the oxygenation curve, for comparison of shapes.

$$Y = \frac{\sum_{i=0}^{4} iK_{4i}[X]^i}{4\sum_{i=0}^{4} iK_{4i}[X]^i} \qquad i = 0, 1, 2, 3, 4 \qquad (1)$$

the Co(II)/Fe(II)-CO system. Furthermore, the stepwise distributions of cooperative free energies for both Co-containing systems were similar to those of normal hemoglobin-binding O_2 (*12*). Systematic oxygenation and CO-binding studies by Yonetani and co-workers (*53, 55*) as well as numerous other studies [such as (*52–54, 64*)] support the concept that the allosteric properties of Co hemoglobin and Co/Fe hybrids closely resemble those of Fe hemoglobin in qualitative behavior, even though the ranges and magnitudes of functional parameters vary.

Energetic distributions for the four resolvable steps of O_2 binding to normal hemoglobin [Fe(II)/Fe(II)-O_2] are entirely consistent with results on the other ligation systems of Table 1. As in the Co(II)/Fe(II)-CO system, species **21** lies closer to species **41** and to the other doubly ligated tetramers than to species **01**. The pH 7.4 distribution, along with known values of ΔG_α and ΔG_β, can be used to predict the tetramer O_2-binding curve in Fig. 3 to within accuracy of its experimental determination (see final Table 1 footnote). The pH 8.9 distribution in Table 1 similarly predicts the experimentally determined O_2-binding curve of Fig. 7 to within experimental accuracy. Shown for comparison is the binding curve for cyanomet hemoglobin predicted by the resolved species distribution at pH 8.8.

Partial resolution of species distributions for the system Fe(II)/Fe(II)-CO have been obtained by Perrella *et al.* (*59*). At pH 7, the energetic spacing of species **21** was estimated to be close to that of the other doubly ligated species, not halfway between the end-states, as had been found in the earliest systems resolved (*6, 8*). The difference in relative placement of species **21** led Perrella *et al.* (*59*) to suggest the possibility of qualitatively different mechanisms for cooperativity in hemoglobins with different heme-site ligands. However, they noted that their results were also entirely consistent with the presence of a third allosteric structure. The subsequent discoveries on energetic distributions in the Co systems with CO and O_2 as ligands (*11, 12*) and on the dramatic plasticity of energetic

Table 1. Free energies (in kilocalories) of dimer-tetramer assembly for intermediate-state hemoglobins in various ligation systems.

Species	Fe(II)/Fe(III)-CN*		Fe(II)/Mn(III)†	Mn(II)/Fe(II)-CO†	Co(II)/Fe(II)-CO‡	Fe(II)/Fe(II)-O_2§	
	pH 7.4	pH 8.8	pH 7.4	pH 7.4	pH 7.4	pH 8.9	pH 7.4
01	−14.4 ± 0.1	−12.7 ± 0.1	−14.4 ± 0.1	−15.6 ± 0.5	−10.6 ± 0.1	−12.4 ± 0.1	−14.4 ± 0.1
11	−11.3 ± 0.2	−10.1 ± 0.2	−11.5 ± 0.3		−9.1 ± 0.2	−10.1	−11.5
12	−11.2 ± 0.2	−10.4 ± 0.2	−10.7 ± 0.3		−8.6 ± 0.4	−10.1	−11.5
21	−11.4 ± 0.2	−10.0 ± 0.3	−11.0 ± 0.3	−13.1 ± 0.5	−8.5 ± 0.2	−8.8	−9.2
22	−8.3 ± 0.2		−7.8 ± 0.3		−7.6 ± 0.4	−8.1	−7.2
23	−8.2 ± 0.2	−9.1 ± 0.2	−7.6 ± 0.3	−7.8 ± 0.5	−7.5 ± 0.2	−8.1	−7.2
24	−8.5 ± 0.2	−9.1 ± 0.2	−8.2 ± 0.3	−8.3 ± 0.5	−7.4 ± 0.1	−8.1	−7.2
31	−8.6 ± 0.2		7.9 ± 0.3		−7.6 ± 0.2	−8.1	−7.2
32	−8.4 ± 0.2	−9.1 ± 0.2	−7.9 ± 0.3		−7.5 ± 0.2	−8.1	−7.2
41	−8.5 ± 0.1	−9.2 ± 0.1	−7.5 ± 0.3	−8.0 ± 0.1	−8.0 ± 0.1	−9.1 ± 0.1	−8.0 ± 0.1

*(*6, 7, 58*). †(*8*). ‡(*11, 12*). §We calculated equilibrium constants for dimer-tetramer assembly from experimentally resolved free energies of the scheme in Fig. 3B at each pH (*42*), assuming the same general distribution pattern as found in the other systems of this table. The value for species **21** was calculated as $^{21}K_2 = 1/2(^2K_2) - {}^{22}K_2 - 1/2(^{23}K_2 + {}^{24}K_2)$, where $^2K_2$ is the experimentally determined composite equilibrium constant and the remaining constants are for species **22, 23,** and **24** (*39*). The latter constants and those of species **31** and **32** were assumed equal to the composite $^3K_2$ determined from experiment. Free-energy values are related to these equilibrium constants through the standard relation $\Delta G = -RT\ln K$ (R, gas constant; T, temperature).

spacings in the cyanomet and O_2 systems (*7, 42*) imply that there is a common general mechanism with a continuum of quantitative manifestations that change with heme-site ligand and conditions. The discrete (or "digital") effects generated by heme-site binding appear to be modulated in a continuous (or "analog") fashion by conditions such as pH.

Identity of the third allosteric structure. The experimentally resolved distribution of cooperative free energies for the cyanomet system at pH 7.4 is incompatible with the concerted two-state MWC model, which requires identical behavior for doubly ligated species (*65*). Also precluded are concerted mechanisms with any number of quaternary structures, such as the three-state concerted mechanism (*66*). Thus, a third "allosteric structure" is required, presumably of the KNF type. Although failure of the purely concerted mechanism is a property of the system as a whole, the focus of interest naturally falls on species **21** and on the two singly ligated species (**11** and **12**) that occupy the intermediate cooperative free-energy levels. Further mechanistic interpretation of the observed free-energy distributions of the ten ligation species requires information on the molecular nature of these species. Do the intermediate allosteric species assume a third quaternary structure, that is, a dimer-dimer interface globally different from those of the two end-states, R and T, or do they reflect cooperativity within the known R and T tetramers?

A solution to this problem came within the past year from studies on the effects of pH and single-site mutations on the energetics of assembly at the $\alpha^1\beta^2$ interface (7). (i) Assembly free energies were determined for 16 hybrid forms of species **21**, each bearing a single mutation site in an α or β subunit across the interface from the ligated dimer. These structurally modified tetramers all exhibited the same 3-kcal cooperative energy found in the normal molecule. The mutationally induced perturbations in assembly free energies were identical to those of species **01** but were uncorrelated with the corresponding perturbations found for species **41.** (ii) At pH 7.4, species **01, 11,** and **21** showed substantial increases of similar

Table 2. Indicators of quaternary structure for the ten ligation species of cyanomet hemoglobin. We resolved all properties of the asymmetric species **11, 12, 21, 22, 31,** and **32** from analyses on hybrid mixtures by using independently resolved species fractions (Fig. 6).

Species	$^{ij}\Delta G_c$* (kcal)	O_2 binding†		−SH reactivity‡	Aromatic CD spectrum§	$\Delta\nu_{H^+}$‖	$\delta\Delta G_{assembly}$¶
		n_{max}	p_{med} (torr)	$t_{1/2}$ (s)			
01	0	3.3	5.3	1000	T	−0.6 ± 0.1	T pattern
11	2.9 ± 0.3	2.0	2.3	550	T	−0.7 ± 0.2	
12	3.2 ± 0.3	2.0	2.3	440	T		
21	3.1 ± 0.3	1.9	5.1	660	T	−0.5 ± 0.3	T pattern
22	6.0 ± 0.3	1.0	0.4	19	R		
23	6.2 ± 0.3	1.2	0.4	17	R	+0.9 ± 0.3	
24	5.9 ± 0.3	1.2	0.5	20	R		
31	5.8 ± 0.3	1.0	0.2	20	R		
32	5.9 ± 0.3	1.0	0.2	17	R	+0.9 ± 0.3	
41	5.9 ± 0.3	n.a.	n.a.	11	R	+0.9 ± 0.1	R pattern

*Cooperative free energies determined from assembly free energies (pH 7.4) of Table 1 (see Fig. 5). †Oxygen-binding data of species **01** are from (*42*). Properties of the partially ligated species were determined from oxygenation isotherms, measured with a Gill cell (*45*), in combination with the median partial pressures of species **11, 12,** and **21,** obtained from cryogenic isoelectric focusing of deoxygenated and oxygenated hybrid mixtures (*10*). The quantity n_{max} is the maximum Hill coefficient (*47*). The quantity p_{med} is the median O_2 concentration (*49*). Conditions were pH 7.4, 21.5°C, and 0.18 M Cl^-. ‡Rates of reaction of β93 cysteine with 4,4′-dithiodipyridine (4-PDS) at 29°C were measured spectrophotometrically at 324 nm (*67, 68*). Assignments of sulfhydryl reactivity rates for hybrid species were based on the amplitudes of kinetic phases and the proportions of parent and hybrid species in solution calculated from the cooperative free energies in column 2. §Circular dichroic spectra (250 to 310 nm) determined on hybrid mixtures and parent species (JASCO-600 spectropolarimeter) at pH 8.0. Spectra of mixtures were deconvolved to obtain component spectra of each species. The CD spectra in this region are a sensitive probe of hemoglobin quaternary structure (*69, 70*). When the tetrameric molecule is switched from the "deoxy" quaternary conformation to the "oxy" form (for example, by completely ligating all four subunits), a significant difference is seen in the CD spectrum. ‖Changes in bound protons in the pH 7.4 to 8.0 region were obtained from values of assembly free energies at pH 7.4, 8.0, and 8.5, calculated as $\Delta\nu_{H^+} = (d\Delta G)/2.3RTdpH$ where $\Delta\nu_{H^+}$ is the change in moles of bound protons per mole of assembly reaction with free energy ΔG. ¶ Assembly free energies for each of 16 single-site mutants or chemically modified hemoglobins were determined for the three ligation species indicated. In species **21** they each contained a single mutation site located across the $\alpha^1\beta^2$ interface from the ligated half-molecule. For each mutant the three forms were studied by cryoisoelectric focusing (*10*) as hybrids in which one of the dimers contained a HbS (β6 Glu→Val) subunit to facilitate electrophoretic resolution. We used deviation free energies determined from equilibrated mixtures of the parent tetramers to calculate the hybrid assembly free energies. Distinctly different patterns of mutational perturbation were found in the species **01** mutants compared to species **41** mutants. Species **21** mutant perturbations were in striking parallel to those of species **01** (*7*).

magnitude in bound protons after assembly (characteristic of quaternary T), whereas the assembly reactions of species **23, 32,** and **41** were each accompanied by proton release characteristic of quaternary R (Table 2). These lines of evidence provided highly consistent results pointing to species **21** as having the quaternary T structure. Species **11, 12,** and **21** thus appear to be quaternary T molecules that differ from species **01** by 3 kcal/mol of free energy; this difference reflects tertiary rather than quaternary structure changes.

Additional indicators of quaternary assignment. Because of the potential importance of these findings to understanding the molecular basis of hemoglobin cooperativity, we carried out a number of additional studies using other kinds of "probes" that are reflective of quaternary structure (Table 2). The responses of T and R tetramers have been characterized extensively in terms of (i) the reactivity of the β93 cysteine to sulfhydryl reagents (*67, 68*), (ii) the circular dichroism (CD) spectrum in the aromatic 280- to 300-nm region (*69, 70*), and (iii) O_2-binding affinities and cooperativities for tetramers partially ligated with cyanomet (*68*). The distribution found among the various ligation species for each of these properties (Table 2) was highly consistent with the results expected on the basis of the assignments of species **01, 11, 12,** and **21** to quaternary T and the remaining species to quaternary R. Although no single type of indicator is entirely conclusive, the composite, which probes different molecular aspects, provides a very strong case.

Symmetry Rule for Quaternary Switching

Assignment of the intermediate species **11, 12,** and **21** to the T quaternary structure along with species **01** provides a simple interpretation of the observed distribution (Table 2) in terms of quaternary switching: switching from T to R occurs whenever a binding step creates a tetramer with one or more ligated subunits (that is, one or more ligated tertiary structures) on each side of the interface that separates the identical dimeric half-molecules, $\alpha^1\beta^1$ and $\alpha^2\beta^2$ (Fig. 2). This "symmetry rule" is satisfied either (i) in going from singly ligated tetramers (species **11** or **12**) to the doubly ligated species **22, 23,** or **24** or (ii) in going from the doubly ligated species **21** to either of the triply ligated species **31** or **32**. Because species **22** can be formed by a single step from either species **11** or **12**, there are a total of six quaternary switchpoints for T-R transition, all of which satisfy the symmetry rule. A switchpoint transition always includes one binding step (without quaternary change) plus a pure quaternary T→R change; however, there are two pairs of these processes at each switchpoint that are energetically equivalent in sum (Fig. 8).

It is reasonable to assume that the symmetry rule for quaternary switching that has been inferred principally from results on cyanomet hemoglobin is also applicable to the other ligation systems. This assumption is supported by CD spectra of species **21** and **24** in the Co-Fe system that indicated T and R quaternary structures, respectively (*71*).

Energetics at the quaternary switchpoints. From a knowledge of the T→R switchpoints and the corresponding free energies of dimer-tetramer assembly it is possible to evaluate the energetic contributions of quaternary and tertiary switching to the cooperative mechanism. The assembly free energies once again provide a "thermodynamic yardstick" by which to gauge these processes, as shown in Fig. 8 for the cyanomet system at pH 7.4.

The assembly free energies and quaternary assignments of species **01** and **41** dictate that the free-energy expenditure along any pathway from $T(t_4)$ to $R(r_4)$ (consisting of four binding steps plus one quaternary transition) would be $(2\Delta G_\alpha + 2\Delta G_\beta + 6)$ kcal/mol. The "thermodynamic distance" between any two tetrameric species can be calculated as the difference between their respective assembly free energies plus the ΔG_α and ΔG_β values for their appropriate binding to dissociated dimers. The pathway of dominant species along **01→11→21→32→41** (Fig. 8) consists of three segments: (i) two binding steps within T, (ii) the switchpoint transition from **21→32**, and (iii) the final binding step **32→41.** The free energy for each segment, calculated from the data of Table 1, is given in brackets. The total 6 kcal/mol of cooperative free energy is found to be spent in equal increments of (i) 3 kcal/mol for sequential cooperativity within T before quaternary transition (the second stepwise binding constant is 170 times the first because binding the second ligand is 3 kcal/mol more favorable) and (ii) 3 kcal/mol for free energy of the switchpoint transition, ΔG_{switch}. This term includes the quaternary T→R switch plus cooperative energy that may accompany the subsequent binding step. Partitioning of the 3 kcal/mol between these two processes cannot be done with present information. However, one does not need to know this partitioning to evaluate the contribution of the switchpoint transition to the distribution of cooperative free energies. In Fig. 8, the 3 kcal/mol has been arbitrarily depicted as pertaining to the T→R quaternary transition. The two other switchpoint transitions in Fig. 8 (**11→22** and **11→23**) also occur with 3 kcal/mol of unfavorable free energy. The energetic criterion for occurrence of a switchpoint transition is that the switchpoint energy barrier (for example, 3 kcal/mol) must

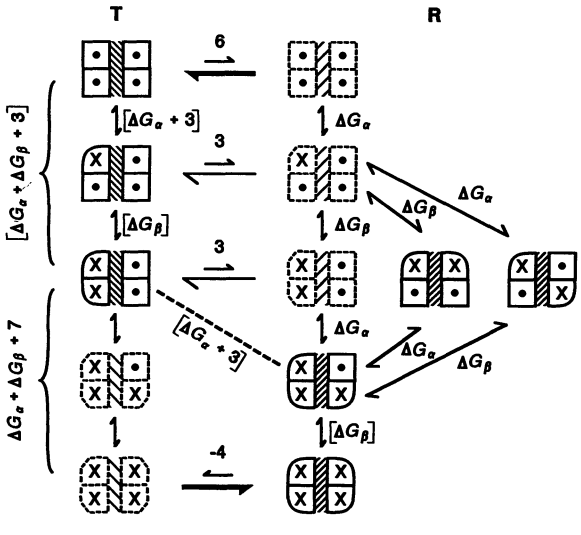

Fig. 8. Cooperative switching for representative tertiary-quaternary combinations of tetramers. Ligated subunits contain an X and have altered shape, symbolic of their conversion to tertiary r. Numerical values in brackets correspond to cyanomet data at pH 7.4 (Table 1). Other numbers represent a plausible scenario consistent with all data. Fully unligated molecules (top) are dominated by $T(t_4)$ and fully ligated molecules (bottom) by $R(r_4)$. At the intermediate states, quaternary structure is controlled by the symmetry rule, leading to dominance of species in solid outline and dense crosshatches. These solid diagrams depict species of the pathway **01→11→21→32→41**, along with species **22** and **23** (far right). The system expends 6 kcal/mol of cooperative free energy (relative to the dissociated subunits) along any pathway between $T(t_4)$ and $R(r_4)$. The expenditure along any path is segmented into a quaternary T→R transition (at one of the six switchpoints) and a sequential cooperativity term at steps within each quaternary structure. Stepwise cooperativity arises when (i) unfavorable free energy from quaternary switching T→R generates a net low-affinity binding step and then a step without quaternary transition (hence, higher affinity) and when (ii) the first binding step within quaternary T is accompanied by unfavorable free energy of tertiary constraint (hence, it has reduced affinity), whereas a subsequent step has reduced (or no) tertiary constraint. The dashed line indicates a switchpoint transition from species **21**(T) to species **32**(R) accompanied by a free energy equal to $\Delta G_\alpha + 3$. Other switchpoint transitions on this diagram include **11**(T)→**22**(R) and **11**(T)→**23**(R), energetically equal to $\Delta G_\beta + 3$ and $\Delta G_\alpha + 3$, respectively. Each pathway through a switchpoint transition sums to $(2\Delta G_\alpha + 2\Delta G_\beta + 6)$ kcal/mol.

be of lower magnitude than the opposing value of intrinsic binding free energy ΔG_α or ΔG_β (for example, −8.3 kcal/mol for O_2 binding).

Sequential Cooperativity Within T and R

The preceding analysis can be extended to evaluate the stepwise cooperativity of tetramers in quaternary T (before the T→R switchover) and also the subsequent cooperativity of tetramers in quaternary R. Cooperative free energies (determined as in Fig. 5) are converted to stepwise terms by successive subtraction. For example, with Co(II)/Fe(II)-CO (Table 1), values along the pathway **01→11→21** are calculated as $^{21}\Delta G_c = (-8.5 + 10.6) = 2.1$ and $^{11}\Delta G_c = (-9.1 + 10.6) = 1.5$; thus, the cooperative free energies are 1.5 and 0.5 kcal/mol for the first and second steps of binding, respectively. The net effect on variation in binding constant is the 0.6 kcal/mol difference between the first and second steps. This difference corresponds to a 2.5-fold increase in binding affinity within quaternary T, as compared to the factor of 170 for corresponding reactions in the cyanomet system. Similarly, one can evaluate the analysis of cooperativity by determining cooperative free-energy values $^{ij}\Delta G_c$ from the assembly free energies of species along any pathway within R. With Co(II)/Fe(II)-CO, the pathway **23→32→41** leads to an increase of affinity of 0.5 kcal/mol for the last step of binding **32→41.**

Tertiary constraint. The quaternary enhancement exhibited by species **23, 24, 31**, and **32** (presumably also species **22**) represents ligand-induced effects within the quaternary R structure. However, the sequential increment of free energy within quaternary R has the opposite sign from that for the T structure. A simple concept for rationalizing these oppositely directed effects of ligand binding is that the tertiary energies are unfavorable (have positive sign) when ligand binding (or unbinding) generates a "mismatch" between tertiary and quaternary structures. The mismatch can occur either by (i) creation of "oxy" tertiary subunits within the deoxy (T) quaternary structure by binding ligands or by (ii) creation of "deoxy" tertiary subunits within the oxy quaternary R structure by bound ligands being released (such as from species **41**). Thus, the observed quaternary enhancement effect in the Co(II)/Fe(II)-CO system may be viewed as the release of unfavorable free energy when the tertiary-quaternary mismatch is eliminated by full ligation of the R tetramer.

An argument implicit in the symmetry constraint of the MWC model was that a mismatch between tertiary and quaternary structures (that is, an r subunit within quaternary T or a t subunit within R) was either sterically forbidden or energetically precluded as a result of the strength of intersubunit bonding (quaternary constraint). Spectroscopic, crystallographic, and computational analyses (*14, 19–24*) indicate that although unfavorable steric effects may be present, they usually do not preclude formation of the heterogeneous tertiary-quaternary combinations. Karplus and co-workers have found that the "allosteric core" of an individual subunit within a tetramer has only two stable positions; one fits without strain into the T structure, the other fits similarly into the R structure (*24*). The new work on intermediates is consistent with these characteristics of the fundamental switching element. It provides an additional step by defining specific cooperativity effects at each end of the ligation sequence that arise from breaking the Monod symmetry constraint. In general, two sequential increments of ligand-induced, positive free energy accompany binding to T, provided the dimer-dimer interface is not crossed. An additional increment occurs when the interface is crossed. In R there appears to be a single increment that corresponds to the first deligation step, with no further change at the second. However, the third deligation generates an additional increment, driving the molecules to T. It is useful to designate these effects "tertiary constraint." "Free energy of tertiary constraint" thus denotes the positive "free energy of tertiary-quaternary mismatch" that generates cooperativity for stepwise ligand binding within quaternary T and also generates (by its release) the free energy of cooperativity for sequential steps within quaternary R.

Cooperativity within dimers. The finding of significant cooperativity for stepwise binding within each dimeric half-tetramer suggests direct structural interaction at the $\alpha^1\beta^1$ contact (such as the G helices of Fig. 2). Such an effect within the tetrameric structure would not in principle conflict with experimental findings that dissociated dimers are noncooperative (*40, 42, 48*). Recent analysis (*72*) indicates significant ligand-linked structural motion at the $\alpha^1\beta^1$ contact that may have a role in the observed $\alpha^1\beta^1$ cooperativity. It is also possible that the apparent dimer cooperativity found in assembled tetramers is an indirect effect that does not involve $\alpha^1\beta^1$ interface changes per se.

Energetic constraints between dimers. The origin of the symmetry rule may be ligand-induced unfavorable interactions between dimeric halves of the molecule (Fig. 8). One can see this interaction by again using thermodynamic cycles to evaluate the free energy of ligating the sites of the second dimer of a molecule on which the first dimer ($\alpha^1\beta^1$) has already bound two ligands. Starting with $T(t_4)$, the free energy of ligating the first dimer is $[\Delta G_\alpha + \Delta G_\beta + 3]$ kcal/mol. Subsequently, the pathway from species **21**(T) to **41**(R) expends an additional 3 kcal/mol plus the intrinsic free energies. To evaluate the cooperative energy term for the path **21**(T)→**41**(T), we only need to know the free energy of the quaternary transition from **41**(R)→**41**(T). Any nonzero value for this term must reflect ligand-induced dimer-dimer interactions within quaternary T, because the free energies for loading the two dimers would then differ. Although the actual magnitude of this dimer-dimer effect is not known, its sign is clearly negative (favoring R). Thus, the binding of two ligands on the first dimer reduces the net affinity for binding at the two sites of the second dimer. An estimate of −4 kcal/mol, based on the inability to switch from R to T caused by organic phosphates (*73*), corresponds to about one-thousandth of the ligand affinity for the second dimer compared to the first. This apparent "negative cooperativity" between halves of the sites in the hemoglobin molecule is similar to behavior observed with certain multisubunit enzymes, in which substrate occupancy of exactly half of the sites reduces or eliminates activity at the identical other half (*74, 75*). The repertoire of hemoglobin as "honorary enzyme" is thus complete except for actual catalytic activity.

A similar effect is present at the switchpoints of singly ligated species (such as in disfavoring species **24** in quaternary T). Ligand-induced negative energetic constraints between dimeric half-molecules may, in fact, be the source of the symmetry rule if such negative cooperativity accompanies "further deligation" of doubly ligated R tetramers, driving them toward T. In general, it is clear that the rules of tertiary-quaternary coupling in hemoglobin tetramers have a hierarchical character.

General mechanism for tetramers. Using the combined information from quaternary indicators and thermodynamic linkages, one can construct a mechanistic picture of tetrameric properties alone, devoid of the assembly reactions that have proved so useful in the elucidation of the energetics of these reactions. This mechanism (Fig. 9) summarizes in general form the results from studies on the four systems of Table 1. Each of the ten ligation species is represented as the dominant quaternary form (T or R). Below each species is a product of equilibrium constants for the various processes that reflect free energy relative to the fully unligated reference species **01.** K_α and K_β are the intrinsic subunit ligand-binding

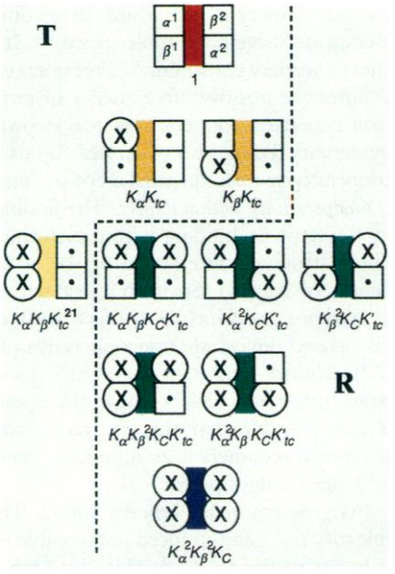

Fig. 9. Allosteric mechanism of hemoglobin. The α and β subunits assume tertiary structures t (depicted as squares) or r (circles), depending on whether the heme-site is unligated (•) or ligated (X). Only the dominant form (R or T) of each ligation species is depicted. The ten species distribute among five cooperative free-energy levels (indicated by colors), reflecting the contributions of concerted and sequential switching elements. Quaternary switching from T to R (separated by dashed line) follows a "symmetry rule" whenever heme-site binding creates a tetramer with at least one ligated subunit on each dimeric half-molecule ($\alpha^1\beta^1$ or $\alpha^2\beta^2$). Energetic levels of dimer-dimer interaction (quaternary constraint) reflect both quaternary structure and sequential cooperativity effects that occur without quaternary change (tertiary constraint). Dimer-dimer interactions are strongest (red) in the unligated tetramer. Binding of two successive ligands within quaternary T reduces quaternary constraint in corresponding increments (to the orange and yellow levels). Quaternary transition to R further diminishes dimer-dimer interactions (to green), whereas the final binding step within R (green to blue) creates an increase in quaternary constraint. The product of equilibrium constants under each species denotes the cumulative energetic weights relative to the unligated species **01** (top). The leftmost combinations of K_α and K_β reflect intrinsic binding to the sites, whereas the remaining terms reflect energetic contributions to cooperativity.

constants, and K_C corresponds to the total cooperative free energy $^{41}\Delta G_c$. K_{tc} and K_{tc}^{21} denote the two levels of tertiary constraint within quaternary T, and K'_{tc} denotes tertiary constraint within quaternary R. Cooperativity within T is thus characterized by the ratio K_{tc}^{21}/K_{tc}. Cooperativity in R occurs when K'_{tc} is less than unity.

This simple model rationalizes all of the tetrameric properties inferred from the work reviewed here and provides a basis for further exploration. Additional studies on the effects of allosteric regulators (protons, organic phosphate, chloride ions, and CO_2) on parameters of the model must be incorporated into its further development.

Conclusions and Outlook

The fundamental switching elements of allosteric proteins were identified over 25 years ago as the ligation-linked sequential and concerted processes of KNF and MWC. Much progress has subsequently been made toward understanding structural aspects of the tertiary and quaternary transitions in the hemoglobin system and the energetic forces driving these transitions. By a strategy developed and implemented during the past 6 years it has been possible to examine, at the level of all ten ligation species, the rules whereby tertiary and quaternary switches are coupled to each other and to evaluate the roles of these switches in the generation of cooperative free energy. What emerges is a specific set of rules, or a "code," that translates the configurational isomers of heme-site ligation into six observed switchpoints of quaternary transition (T to R). Central to this code are three concepts: (i) the configuration of ligated heme-sites within the tetramer is an essential factor in controlling quaternary structure, (ii) sequential cooperativity is manifested within each quaternary structure as a result of unfavorable free energies arising from tertiary-quaternary mismatch, and (iii) the effects of tertiary-quaternary mismatch are hierarchical, leading not just to sequential cooperativity within each dimer but also to overall dimer-dimer anticooperativity, which produces the observed symmetry rule.

The hemoglobin mechanism can be viewed as a cascade of parallel "sequential" (KNF) reactions that contain concerted transitions nested within the six switchpoint transitions. Equivalently, it may be viewed as a concerted T→R framework with sequential cooperativity nested inside the R and T manifolds. In limiting cases the system approaches a pure KNF or a pure MWC mechanism. However, the specific rules for tertiary-quaternary coupling revealed by the recent work on intermediate states supersede either of these overly simplified mechanisms.

The new findings provide a framework for further testing and exploration of the detailed, atomic-level origins of the allosteric mechanism in structural and energetic terms. Current studies of mutant hemoglobins in partially ligated states and of the effects of allosteric modifiers appear promising. As the hemoglobin molecule continues to be a prototype for attempts to understand other multimeric protein switches, studies of the intermediate species in those systems may also reveal new "mechanistic secrets."

REFERENCES AND NOTES

1. J. Monod, *Chance and Necessity* (Collins, London, 1972).
2. J. T. Edsall, *J. Hist. Biol.* **5**, 205 (1972).
3. J. Monod, J. Wyman, J.-P. Changeux, *J. Mol. Biol.* **12**, 88 (1965).
4. D. E. Koshland, G. Nemethy, D. Filmer, *Biochemistry* **5**, 364 (1966).
5. M. F. Perutz, *Q. Rev. Biophys.* **22**, 139 (1989).
6. F. R. Smith and G. K. Ackers, *Proc. Natl. Acad. Sci. U.S.A.* **82**, 5347 (1985).
7. M. A. Daugherty *et al.*, *ibid.* **88**, 1110 (1991).
8. F. R. Smith, D. Gingrich, B. Hoffman, G. K. Ackers, *ibid.* **84**, 7089 (1982).
9. G. K. Ackers and F. R. Smith, *Annu. Rev. Biophys. Biophys. Chem.* **16**, 583 (1987).
10. V. J. LiCata, P. C. Speros, E. Rovida, G. K. Ackers, *Biochemistry* **29**, 9772 (1990).
11. P. C. Speros, V. J. LiCata, T. Yonetani, G. K. Ackers, *ibid.* **30**, 7254 (1991).
12. M. L. Doyle *et al.*, *ibid.*, p. 7263.
13. M. F. Perutz, *Nature* **228**, 726 (1970).
14. J. Baldwin and C. Chothia, *J. Mol. Biol.* **129**, 175 (1979).
15. A. M. Lesk, J. Janin, S. Wodak, C. Chothia, *ibid.* **183**, 267 (1985).
16. R. E. Dickerson and I. Geis, *Hemoglobin Structure, Function, Evolution, and Pathology* (Benjamin-Cummings, Menlo Park, CA, 1983).
17. In this article we use quaternary in the crystallographic sense, that is, to denote distinctly different ways of packing the two αβ dimers within the tetramer (Fig. 2). If intersubunit bonds are altered within one of these packing motifs, we do not consider that a new quaternary structure exists. A third quaternary structure has recently been found in the mutant human hemoglobin Ypsilanti that conforms to the crystallographic definition [F. R. Smith, E. E. Lattman, C. W. Carter, *Proteins* **10**, 81 (1991)].
18. The symmetry constraint of the MWC model, requiring $T(t_4)$ and $R(r_4)$ as the only tertiary-quaternary combinations, is not required for the model's mathematical formulation. See C. Debru, *Biophys. Chem.* **37**, 15 (1990).
19. A. Brzozowski *et al.*, *Nature* **307**, 74 (1984).
20. A. Arnone, P. Rogers, N. V. Blough, J. L. McGourty, B. M. Hoffman, *J. Mol. Biol.* **188**, 693 (1986).
21. R. Luisi, B. Liddington, G. Fermi, N. Shibayama, *ibid.* **214**, 7 (1990).
22. S. Ogawa and R. G. Shulman, *ibid.* **70**, 315 (1972).
23. R. G. Shulman, J. J. Hopfield, S. Ogawa, *Q. Rev. Biophys.* **8**, 325 (1975).
24. R. R. Gelin, A. W. Lee, M. Karplus, *J. Mol. Biol.* **171**, 489 (1983).
25. M. F. Perutz, *Nature* **228**, 734 (1970).
26. A. Szabo and M. Karplus, *J. Mol. Biol.* **72**, 163 (1972).
27. J. Herzfeld and E. Stanley, *ibid.* **82**, 231 (1974).
28. G. K. Ackers and M. L. Johnson, *ibid.* **147**, 559 (1981).
29. A. Lee and M. Karplus, *Proc. Natl. Acad. Sci. U.S.A.* **80**, 7055 (1983).
30. M. L. Johnson, B. W. Turner, G. K. Ackers, *ibid.* **81**, 1093 (1984).
31. G. Viggiano and C. Ho, *ibid.* **76**, 3673 (1979).
32. L. W. M. Fung, A. P. Minton, C. Ho, *ibid.* **73**, 1581 (1976).
33. S. Miura and C. Ho, *Biochemistry* **21**, 6280 (1982).
34. ———, *ibid.* **23**, 2492 (1984).
35. S. Miura, M. Ikeda-Saito, T. Yonetani, C. Ho, *ibid.* **26**, 2149 (1987).
36. G. Louie, J. J. Englander, S. W. Englander, *J. Mol. Biol.* **201**, 765 (1988).
37. R. W. Noble, *ibid.* **39**, 479 (1969).
38. G. Weber, *Biochemistry* **11**, 864 (1972).
39. G. K. Ackers and H. R. Halvorson, *Proc. Natl. Acad. Sci. U.S.A.* **71**, 4312 (1974).
40. F. C. Mills, M. L. Johnson, G. K. Ackers, *Biochemistry* **15**, 5350 (1976).

41. F. C. Mills and G. K. Ackers, *Proc. Natl. Acad. Sci. U.S.A.* **76**, 273 (1979).
42. A. H. Chu, B. W. Turner, G. K. Ackers, *Biochemistry* **23**, 604 (1984).
43. D. W. Pettigrew *et al.*, *Proc. Natl. Acad. Sci. U.S.A.* **79**, 1849 (1982).
44. K. Imai, *Allosteric Effects in Hemoglobin* (Cambridge Univ. Press, Cambridge, MA, 1982).
45. D. Dolman and S. J. Gill, *Anal. Biochem.* **87**, 127 (1978).
46. M. E. Anderson, J. K. Moffat, Q. H. Gibson, *J. Biol. Chem.* **246**, 2796 (1971).
47. The most popular index of cooperativity is the Hill coefficient, n. For a binding curve Y (fraction of occupied sites) versus x (unbound ligand concentration), the Hill coefficient $n = d\log[Y/(1 - Y)]/d\log x$ provides a measure of cooperativity in terms of statistical variance of the species population. See J. T. Edsall and H. Gutfreund, *Biothermodynamics* (Wiley, New York, 1984), p. 201. Another common index is the Wyman interaction energy [J. Wyman, *Adv. Protein Chem.* **18**, 223 (1964)], which is the difference between free energies of binding of the last and first ligands. Both of these indexes are readily calculable from a knowledge of the linkage free energies of Fig. 3B.
48. D. Atha, M. L. Johnson, A. F. Riggs, *J. Biol. Chem.* **254**, 12390 (1979).
49. J. Wyman and S. J. Gill, *Binding and Linkage* (University Science, Mill Valley, CA, 1990).
50. Transient kinetics of oxygenated hemoglobins have almost always been analyzed under the constraint of a two-state MWC mechanism; compare with J. Hofrichter *et al.*, *Biochemistry* **30**, 6583 (1991).
51. B. M. Hoffman and D. H. Petering, *Proc. Natl. Acad. Sci. U.S.A.* **67**, 637 (1976).
52. K. Moffat, R. S. Loe, B. M. Hoffman, *J. Mol. Biol.* **104**, 669 (1976).
53. T. Yonetani, H. Yamamoto, G. V. Woodrow, *J. Biol. Chem.* **249**, 682 (1974).
54. N. V. Blough, H. Zemel, B. M. Hoffman, T. C. K. Lee, Q. H. Gibson, *J. Am. Chem. Soc.* **102**, 5683 (1980).
55. K. Imai, M. Ikeda-Saito, T. Yonetani, *J. Mol. Biol.* **138**, 635 (1980).
56. J. F. Deatherage, R. S. Loe, C. M. Anderson, K. Moffat, *ibid.* **104**, 687 (1976).
57. M. Perrella and L. Rossi-Bernardi, *Methods Enzymol.* **76**, 133 (1981).
58. M. Perrella, L. Benazzi, M. A. Shea, G. K. Ackers, *Biophys. Chem.* **35**, 97 (1990).
59. M. Perrella, A. Colosimo, L. Benazzi, M. Ripamonti, L. Rossi-Bernardi, *ibid.* **37**, 211 (1990).
60. M. Samaja, E. Rovida, M. Niggeler, M. Perrella, L. Rossi-Bernardi, *J. Biol. Chem.* **262**, 4528 (1987).
61. S. A. Fowler, J. Walder, A. DeYoung, L. D. Kwiatkowski, R. W. Noble, *Biochemistry*, in press.
62. G. K. Ackers, *Adv. Protein Chem.* **24**, 323 (1970).
63. M. A. Daugherty and G. K. Ackers, unpublished results.
64. J. C. W. Chien and F. W. Snyder, *J. Biol. Chem.* **251**, 1670 (1976).
65. G. K. Ackers, *Biophys. Chem.* **37**, 371 (1990).
66. A. P. Minton and K. Imai, *Proc. Natl. Acad. Sci. U.S.A.* **71**, 1418 (1974).
67. R. S. Ampulski, V. E. Ayer, S. D. A. Morell, *Anal. Biochem.* **32**, 163 (1969).
68. M. L. Doyle and G. K. Ackers, unpublished results.
69. M. F. Perutz, J. E. Ladner, S. R. Simon, C. Ho, *Biochemistry* **13**, 2163 (1974).
70. M. F. Perutz, A. R. Fersht, S. R. Simon, G. C. K. Roberts, *ibid.*, p. 2174.
71. D. Myers, M. A. Daugherty, G. K. Ackers, unpublished results.
72. G. Rose, B. Zimm, L. TenEyck, and W. Nichols have analyzed subunit motions using difference plots that map changes in interresidue α-carbon distances between deoxy and oxy crystallographic structures. Surprisingly, they find significant changes within the αβ dimer.
73. M. C. Marden, B. Bohn, J. Kister, C. Poyart, *Biophys. J.* **57**, 397 (1990).
74. A. Levitzki, W. B. Stallcup, D. E. Koshland, *Biochemistry* **10**, 3371 (1971).
75. A. R. Fersht, R. S. Mulvey, G. L. E. Koch, *ibid.* **14**, 13 (1975).
76. We thank T. Yonetani and B. Hoffman for metal-substituted hemoglobin samples and M. Perrella for advice on cryogenic separation techniques, all of which have been crucial to our studies on the intermediate states cooperativity problem. We thank R. L. Baldwin, H. F. Bunn, J. T. Edsall, I. Geis, C. Ho, E. E. Lattman, D. Powers, A. Riggs, G. Rose, H. K. Schachman, and B. Zimm for helpful comments on earlier drafts of this article. Our work has been supported by NIH grants R37-GM24486 and PO1-HL40453 and by NSF grant DMB 9107244.

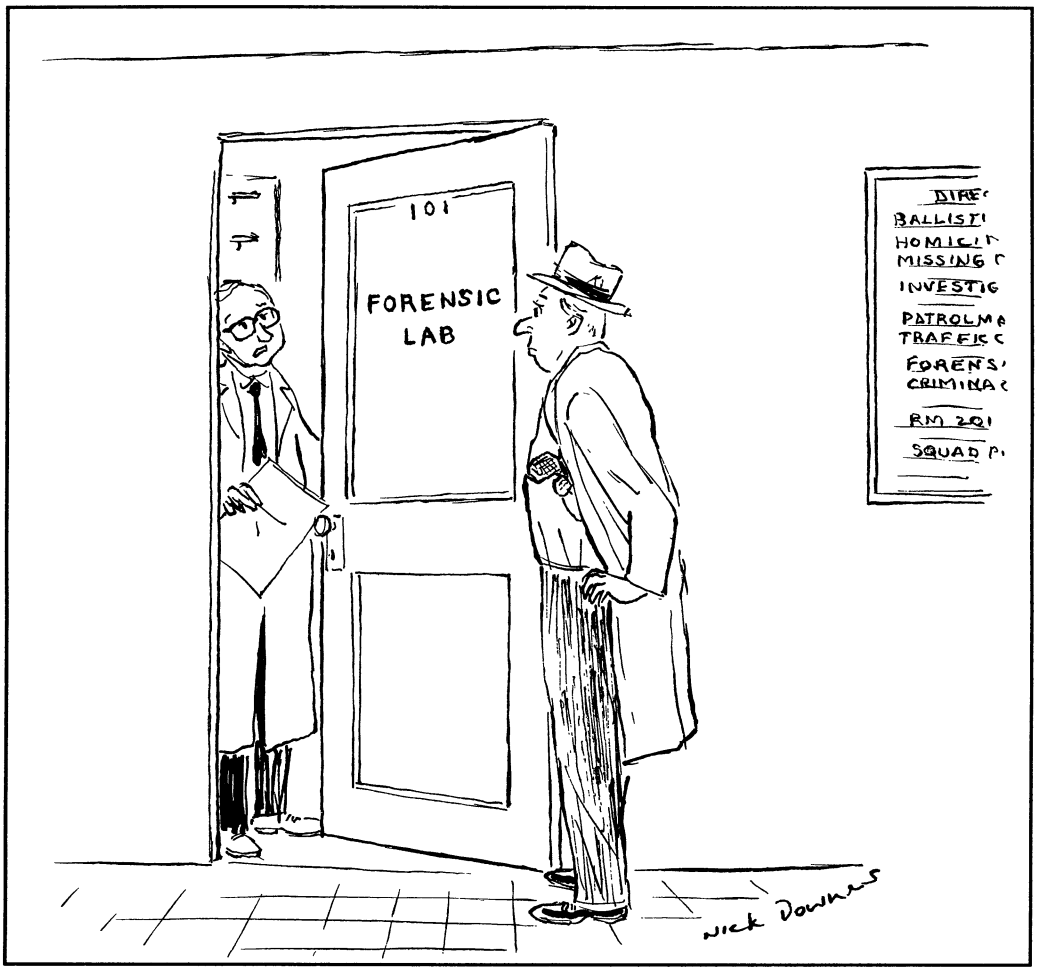

"The metallurgical, instrumental, elemental, microscopic, and laser light analyses say the butler did it."